WRF Visitors Program Report
Evaluation of WRF model improvements with novel boundary-layer observations - Focus on diurnal cycle and stable boundary layer

G.J. Steeneveld*, O.K. Hartogensis*, A.F. Moene*, H. Klein Baltink+, and A.A.M. Holtslag*
*Wageningen University, Wageningen, The Netherlands. +Royal Netherlands Meteorological Institute, De Bilt, The Netherlands

Summary

Boundary-layer schemes play a key role in the forecasting of the diurnal cycle of the thermodynamic variables and atmospheric compounds. Due to the strong and complex coupling between turbulence and radiation, boundary-layer representations of the nocturnal boundary layer perform rather poorly in mesoscale models. We critically evaluate the representation of the stable boundary layer and diurnal cycle over land in WRF. First, we evaluate the performance of the WRF atmospheric boundary-layer schemes with detailed surface and upper air observations from CASES-99 for three contrasting diurnal cycle. In addition, we compare the WRF output with those from the mesoscale models MM5, COAMPS, and HIRLAM. In order to extend the comparison to cover different conditions, we propose to evaluate WRF against a network of high resolution (both spatial and in time) in-situ observations (ceilometer, scintillometry) in the Netherlands, including Cabauw tower observations. Finally, an alternative scheme for the stable nocturnal boundary layer has been implemented in WRF and tested. Recent research carried out at our group has shown a large improvement in the calculation of the thermodynamic variables after introducing a vegetation layer and reduced turbulent mixing.

1. Introduction

Mesoscale models such as WRF and MM5 are used for operational short-range regional weather forecasting, to predict air pollution episodes (Hanna and Yang, 2001; Tie et al., 2007), to reconstruct regional budgets of several trace gases (Denning et al., 2008), e.g. CO_2, and for atmospheric research. It is important for many applications that mesoscale models predict the profiles of potential temperature, specific humidity, trace gases and wind speed and direction, in combination with surface turbulent and radiation fluxes, correctly.

Therefore, the relevant physical processes in the atmospheric boundary layer (ABL) should be included in those models (Teixeira et al., 2008). In mid-latitudes, the ABL undergoes a clear 24 hour cycle. During daytime the ABL gets well mixed by convective eddies that transport heat, moisture and scalars upward from the surface. On the contrary, during nighttime, the ABL has strong vertical gradients in wind speed and temperature. In addition to turbulent mixing, the impact of radiation divergence (e.g. Ha and Mahrt, 2003) and the feedback with the underlying soil is also evident for stable conditions (Holtslag and De Bruin; 1988). Furthermore, a low-level jet can develop during nighttime (e.g. Song et al., 2005). Generally, the structure and modeling of the stable boundary layer (SBL) is more complicated and variable than the daytime ABL (Mahrt, 1999).

Evaluation of atmospheric flows simulated by mesoscale models (i.e. WRF, MM5) has shown that the results are strongly dependent on the ABL scheme used. During daytime the modeled ABL typically is too shallow as compared with observations (e.g., Holtslag, et al. 1995, Vila et al., 2004). Consequently, the modeled boundary layer is characterized by lower values of the (potential) temperature and higher values of the specific humidity and mixing ratios of greenhouse gases. Under nocturnal conditions, the model results show the difficulty to predict the minimum temperature and peak greenhouse gas concentrations close to the surface as a result of too much mixing (e.g. Beljaars and Viterbo, 1998, King et al, 2001, Beare et al, 2006, Steeneveld et al., 2006, 2008). Together this results in an underestimation of the forecasted diurnal temperature range, especially for weak winds. Also, the nocturnal wind maximum (low-level jet) is not well represented, as is the morning transition.

Most of the recently published ABL parameterization improvements are not yet implemented in

mesoscale models like WRF, which hampers the quality of these models for practical applications and scenario studies. Given the poor quality of the current representations of the surface heat fluxes and the ABL in atmospheric models, there is an urgent need for improvement and evaluation on the scale of the model grid box (order of 5 to 50 km.).

Despite the problems mentioned above, Steeneveld et al. (2006) showed that the diurnal cycle can be modeled satisfactorily on a local scale when all physical processes are included, and both the external large-scale forcings (advection, geostrophic wind speed) and soil properties are known accurately. Steeneveld et al. (2007) also showed that the representation of the diurnal temperature range, minimum temperature and boundary-layer profiles of MM5-MRF can be improved. This can be achieved with the incorporation of a (vegetation) layer of small heat capacity at the surface, and the introduction of ABL scheme with limited mixing at night. This model improvement has large impact on the ability to forecast frost and fog.

The reported research will focus on the evaluation and model improvement of WRF for the nighttime. This will be done against novel boundary-layer observations with high spatial (both horizontal and vertical) and temporal resolution for two different areas. State of the art insights and parameterizations (Steeneveld et al., 2006, 2008) will be implemented in WRF and evaluated under various atmospheric conditions.

2. Method and Research Questions

The main objectives mentioned above will be achieved as follows. The WRF model will be configured for an area of 1500 * 1500 km for the two study areas, using a nesting up till a horizontal resolution of a about 1 km around the observational sites. The NCAR-FNL will provide initial conditions and boundary conditions every 6 hours. Since we aim to evaluate model performance we do not apply any data assimilation. One day will be used for spin up time. In addition, we will alter the land use properties in the model as close to the observed values.

Our strategy is to evaluate the model forecasts for turbulent and radiative fluxes near the surface, for boundary-layer height, for surface temperature and humidity, and for atmospheric profiles of thermodynamic variables. Also the critical aspects of the stable boundary layer will be examined. The final step is the implementation of a new ABL scheme for the stable boundary layer. The specific objectives are:

1. Critical evaluation of WRF for the diurnal cycle of the atmospheric boundary layer for three contrasting days in CASES-99 (23-26 Oct. 1999). These days are a series of “golden days” with low, medium large geostrophic wind speed. We will also compare WRF with model forecasts from MM5, COAMPS and HIRLAM. The latter simulations have already been done and are available (Steeneveld et al., 2008). This case is currently examined by the ABL community in the GEWEX Atmospheric Boundary Layer Study (GABLS, Svensson and Holtslag, 2006; http://www.misu.su.se/~gunilla/gabls/).

2. Finally we implemented a new ABL scheme for the stable boundary layer over land in WRF (as was done in Steeneveld et al., 2008 for MM5-MRF), and evaluate this at first instance for a series of “golden days” during the CASES-99 field campaign.

3. Evaluation of the atmospheric boundary-layer schemes in WRF with a network of novel in-situ measurements in The Netherlands, including Cabauw tower observations, a ceilometer, radar and a network of scintillometers. Herein we will specifically focus on the representation of the diurnal cycle and the stable boundary layer.

3. RESULTS

PART 1: GABLS/ CASES-99

a) CASES-99 Observations

The CASES-99 measurement campaign was organized to study the relevant processes in the stable boundary layer and to improve ABL model parameterizations (Poulos et al., 2002;

http://www.cora.nwra.com/cases/CASES-99.html). The experiment was conducted near Leon, Kansas, U.S.A. (37.6486º N, -96.7351º E, 436 m ASL) and lasted from 1-31 October 1999. The area consists of relatively flat homogeneous terrain of prairie grassland with a relatively dry soil.

Ground based observations consist of profiles of temperature, humidity and wind along a 60 m tower, and turbulent and radiative fluxes near the surface. In addition, the soil heat flux was measured with great detail. Hourly launched radiosondes provided information on the structure of temperature, wind speed and direction above 60 m AGL. Wind speed structure below 200 m was also obtained with sodar and aloft with a tethered balloon. In addition to the observation at the central main site, also spatial information is available from 10 m towers at 300, 900, and 1800 m around the central site, plus the routine observations by the ABLE project (approximately 30 km from the central site). As such, this dataset is a very complete and innovative for model evaluation and improvement.

b) Synoptic conditions

We have selected a three day period: 23 Oct. 1999 00.00 UTC – 26 Oct 1999 18.00 UTC. The three selected nights have a moderate, strong and very weak synoptic forcing respectively. During the first night the CASES-99 site is located under a high-pressure system with a geostrophic wind speed ~6 ms^{-1}. The near surface turbulence is of intermittent character during this night. During the second night a trough is west of the measurement site, which coincides with increasing geostrophic forcing in time and heat advection. At about 200 m AGL a typical Great Plains LLJ of 21 ms^{-1} was observed (Banta et al., 2002). A weak front passes at the end of the night, which was most clearly seen in the q increase from ~2.5 to ~6 g kg^{-1}, although no clouds were observed. In the last night, the site is under a high pressure area, and the geostrophic wind speed is about 4 ms^{-1}, and decreases at night. Advection is absent and radiative cooling plays an important role in the SBL during this night.

c) Model configuration

The limited are models are run for a 1620 km x 1620 km area over the central part of the U.S.A. WRF, MM5 and COAMPS use 31 x 31 grid points with a grid spacing in the outer domain of 54 and 49 km respectively. Three smaller domains (also 31 x 31 nodes) with a resolution of 18, 6 and 2 km are nested inside this domain to avoid model errors from coarse resolution. HIRLAM uses 10 km horizontal resolution without nesting in the whole domain, covering nearly the entire U.S.A. Although the three models do not have exactly the same horizontal resolution, they all use a very high resolution. Since land-surface properties are rather homogeneous in this region, significant improvement from increased resolution should not be expected. This was confirmed from coarse grid MM5 and COAMPS simulations, where the results from the 2 and 6 km nests are nearly identical.

The U.S. Geological Survey provides the land surface characteristics (Zehnder, 2002). We used the locally observed values for z_0 (0.03 m) and the soil moisture availability (M = 0.08), for the relevant land-use types. MM5 employed 36 terrain following σ_p-levels (22 layers are in the lowest 2 km), COAMPS used 50 σ_z-levels, and HIRLAM 40 hybrid layers. Initial and boundary conditions for atmospheric variables are taken from the ECMWF (1º x 1º) operational analysis every 6 hours. No data-assimilation of surface and upper air observations has been performed during the simulations, and the models use a 24 h spin-up. We will analyze the period of 23 Oct 1800 UTC to 26 Oct 1800 UTC.

Regarding the boundary layer physics in WRF, we use the so-called MRF scheme (Troen and Mahrt, 1986; Hong and Pan, 1996) which utilizes a prescribed cubic eddy diffusivity profile with height, with the magnitude depending on the characteristic velocity scale at the surface layer. This scheme allows for non-local heat transport during the day. This extension is needed to represent transport by large eddies on the scale of the ABL itself, instead of local transport. A well-known drawback of this widely used scheme is excessive daytime ABL top entrainment, and overestimation of the turbulent transport at night (e.g. Vila et al., 2002; Steeneveld et al., 2008). The 2nd scheme is an extension MRF, (so called YSU). The extensions consist of a) inclusion of prescribed entrainment rate at the ABL top, b) non-local transport of momentum, and c) Prandtl number (K_M/K_H) depending on height (see also Noh et al., 2003). As such, we will evaluate whether these modifications circumvent the deficiencies in the MRF scheme. Finally the 3rd scheme is a 1.5 order closure scheme (MYJ) and uses a prognostic equation for the turbulent kinetic energy (see Stull, 1988; Steeneveld et al., 2008). Then the eddy diffusivity is determined by multiplication of the turbulent kinetic energy and a length scale.

d) Results

Steeneveld et al. (2008) evaluated the MM5, HIRLAM and COAMPS model against CASES99 observation for different atmospheric conditions. Inclusion of the WRF model results for the same case studies would provide an extremely useful as a benchmark. Fig 1 shows the model results, in black for the original study in Steeneveld et al. (2008) and in gray for WRF2.2. Fig 1a shows that WRF models the net radiation that is comparable to MM5, and with the observations. The similar holds for the longwave downwelling radiation. On the other hand, substantial differences between MM5 and WRF occur for the turbulent fluxes. During daytime all schemes perform well on sensible heat flux. However, during the windy night, the WRF-MYJ has a substantially larger sensible heat flux than the other models and the observations. In more detail Fig. 1g shows that also for the radiative night H has a magnitude that is too large, and that the intermittent behaviour in the first night is missing in the model forecast.

The latent heat flux during daytime is small and well modeled, except that the WRF-MYJ scheme overestimates daytime L_vE, as did the MM5-ETA scheme. During nighttime, all scheme provide slightly too much evaporation, compared to the observations, especially in the second night. Friction velocity, an indicator for turbulent intensity compares well with the other model schemes, except that WRF-MYJ u_* is slightly smaller than for MM5-ETA.

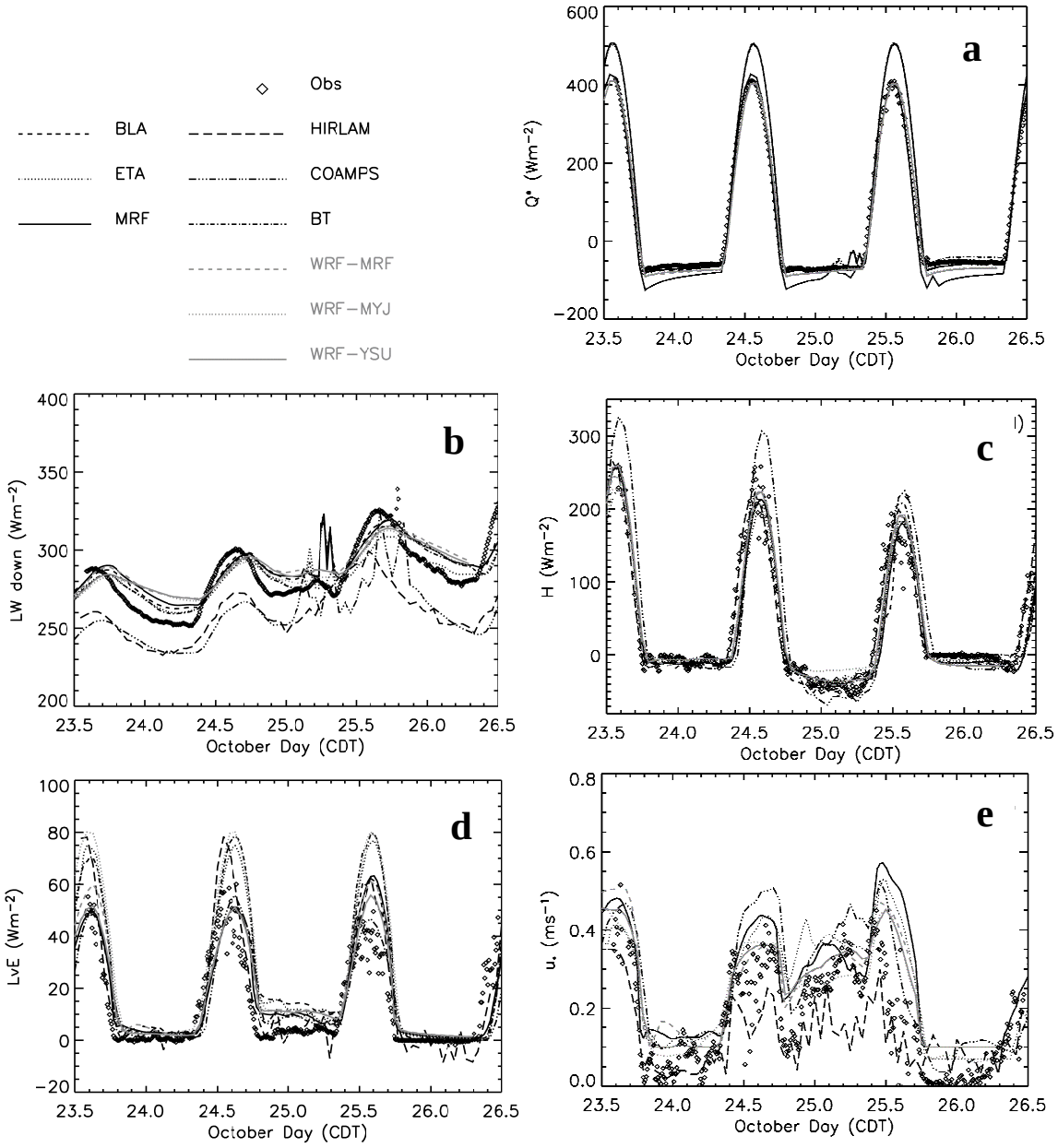

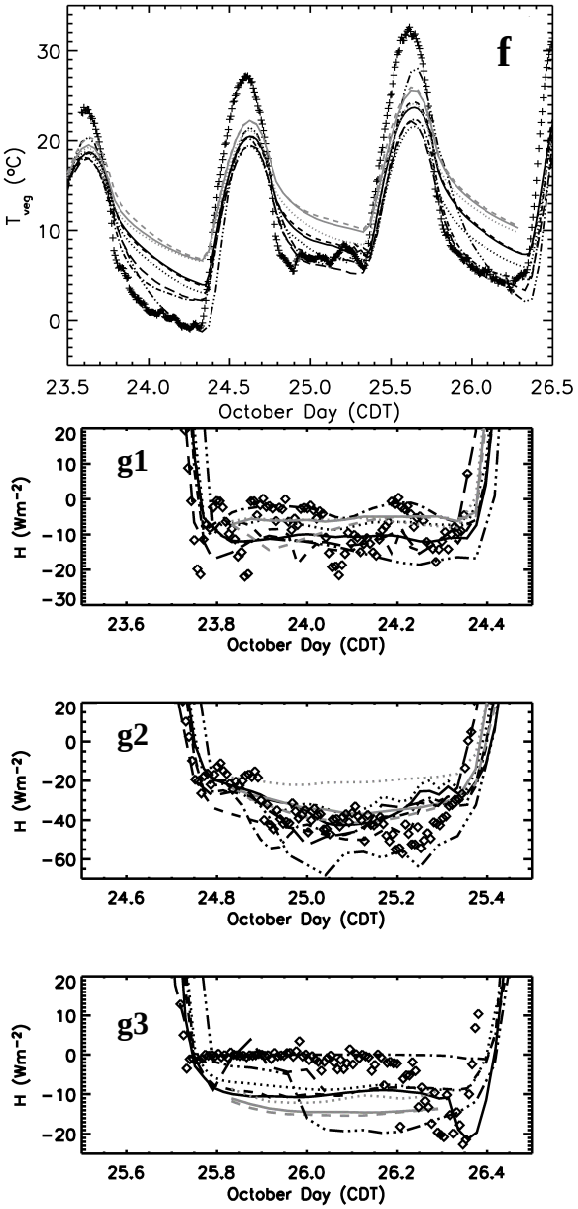

Fig. 1: Modeled and observed net radiation (a), longwave downwelling radiation (b), sensible heat flux (c), latent heat flux (d), friction velocity (e), surface temperature (f), and nocturnal sensible heat flux (g).

The WRF model deficiencies are similar as in MM5: friction velocity is overestimated and drop of u* from the first day toward the night is substantially underestimated. This may impact on the representation of the low-level jet.

Fig. 2 shows that the WRF results for θ and q are consistent with earlier findings in MM5: the MYJ scheme produces shallow PBLs that are too cold and too humid during the day. WRF-YSU and WRF-MRF produces deeper and warmer PBLs than MM5-MRF. However, the inversion is slightly sharper with WRF. As a whole, WRF results fit well in the spread of the model results, and are closer to the observations than the ensemble of the other models, especially for humidity. Fig 3 shows that the WRF has problems with representing the low-level jet at night. WRF-MYJ shows the best performance, closely followed by WRF-YSU. As such the model updates in the WRF-YSU scheme seems to be beneficial for LLJ forecasting compared to MRF (see also part III).

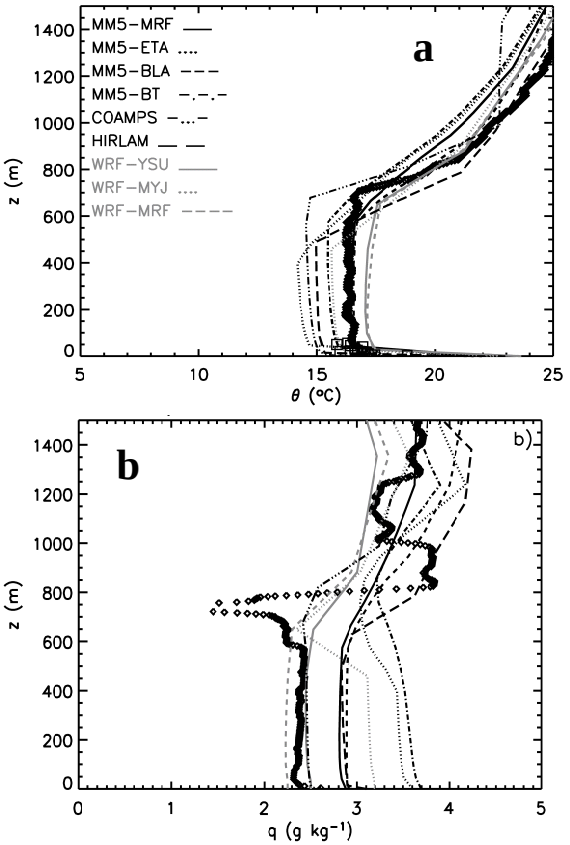

Fig. 2: Modeled & observed potential temperature & specific humidity for 24 Oct 1999, 1900 UTC.

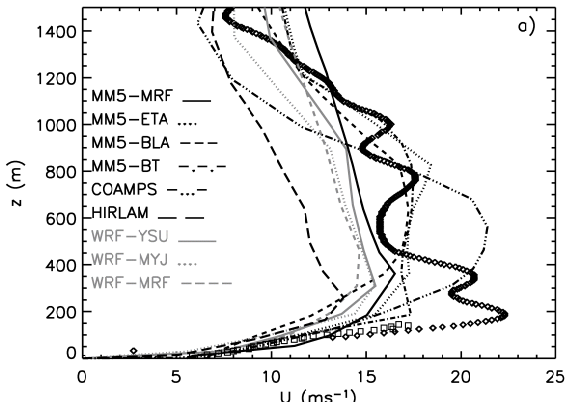

Fig. 3: Modeled and observed wind speed for 25 Oct 1999, 1100 UTC.

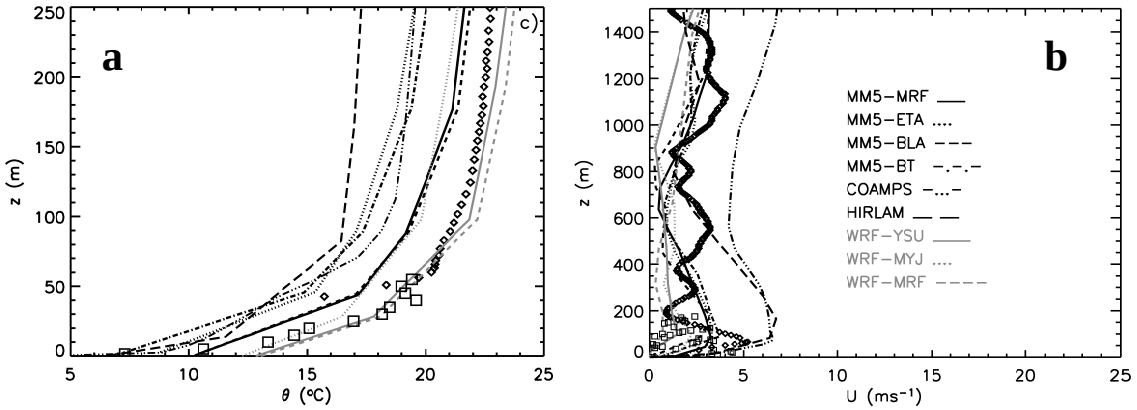

Fig. 4: Modeled and observed potential temperature (a) & wind speed (b) for 26 Oct 1999, 1100 UTC.

Fig. 4a shows that for calm nighttime conditions, WRF forecasts a similar profile structure as most other models, and WRF is closer to the observations than the other models. However, near the surface WRF is missing a strong and sharp inversion (corresponding problem in other models). As such it seems that further attention should be paid to model parameterizations that govern the nighttime boundary layer, i.e. surface layer, boundary layer, the land-surface scheme, but also the radiation schemes (although longwave radiation was well forecasted in these runs). The observed modest LLJ in Fig 4b is not found with WRF, as in most of the model runs, although WRF-MYJ shows a bit of a LLJ like structure. In addition, one may consider that more vertical resolution than usually applied is needed to resolve the stable boundary layer (amongst others Raisanen 1996, Steeneveld et al., 2006).

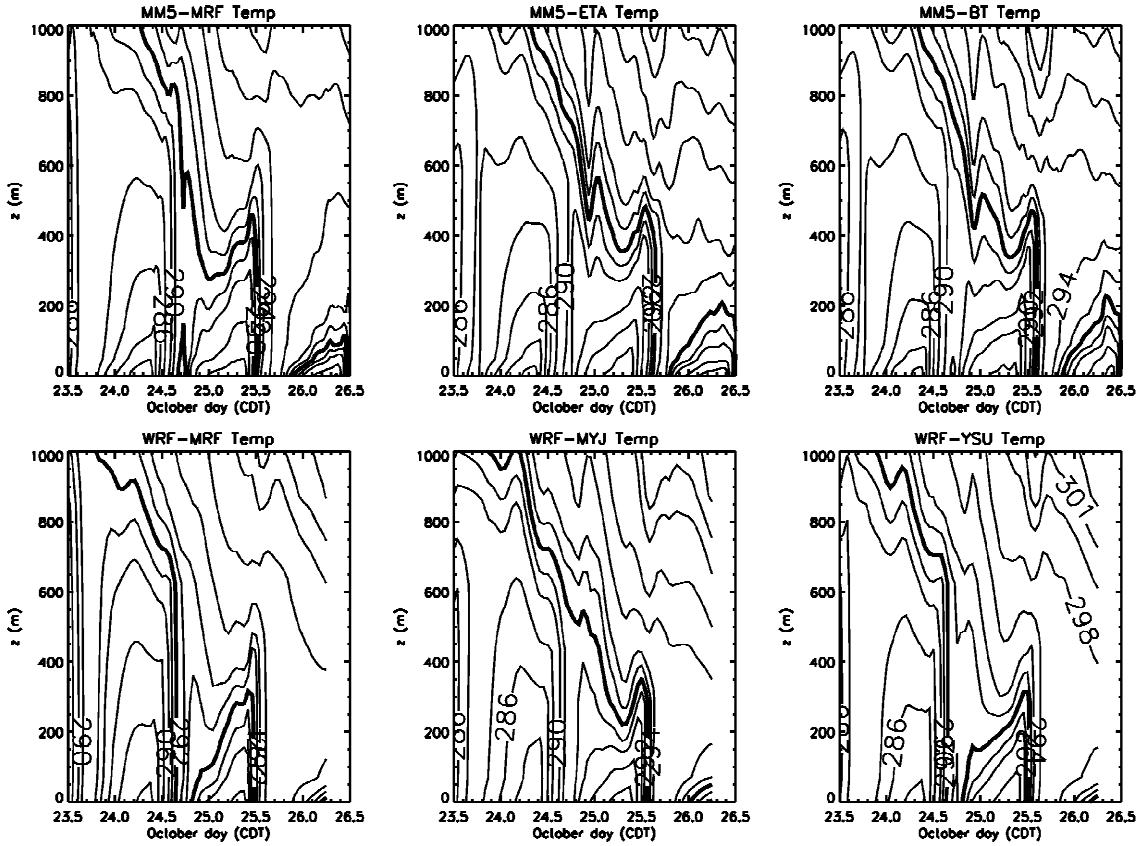

Fig 5a: Contour plots of potential temperature for different schemes in WRF and MM5. For COAMPS and HIRLAM these plots can be found in Steeneveld et al. (2008).

Fig. 5a show contour plots of time series of modeled potential temperature for three schemes in WRF and compared with MM5 results. WRF results are similar as MM5 results, except that the WRF results are

warmer than MM5. WRF-MRF and WRF-YSU show a nighttime cooling that is more slow in calm nights than in their MM5 counterpart. Also, it seems that MM5-ETA resolves the daytime ABL top sharper than WRF-MYJ.
In Fig 5b the spatial-temporal development of the wind speed is shown. The general wind pattern is similar as in MM5, especially for the first night. For the second night WRF produces low-level jets that are less pronounced and less sharp, and with a lower wind speed than in MM5, especially for MM5-ETA vs. WRF-MYJ.

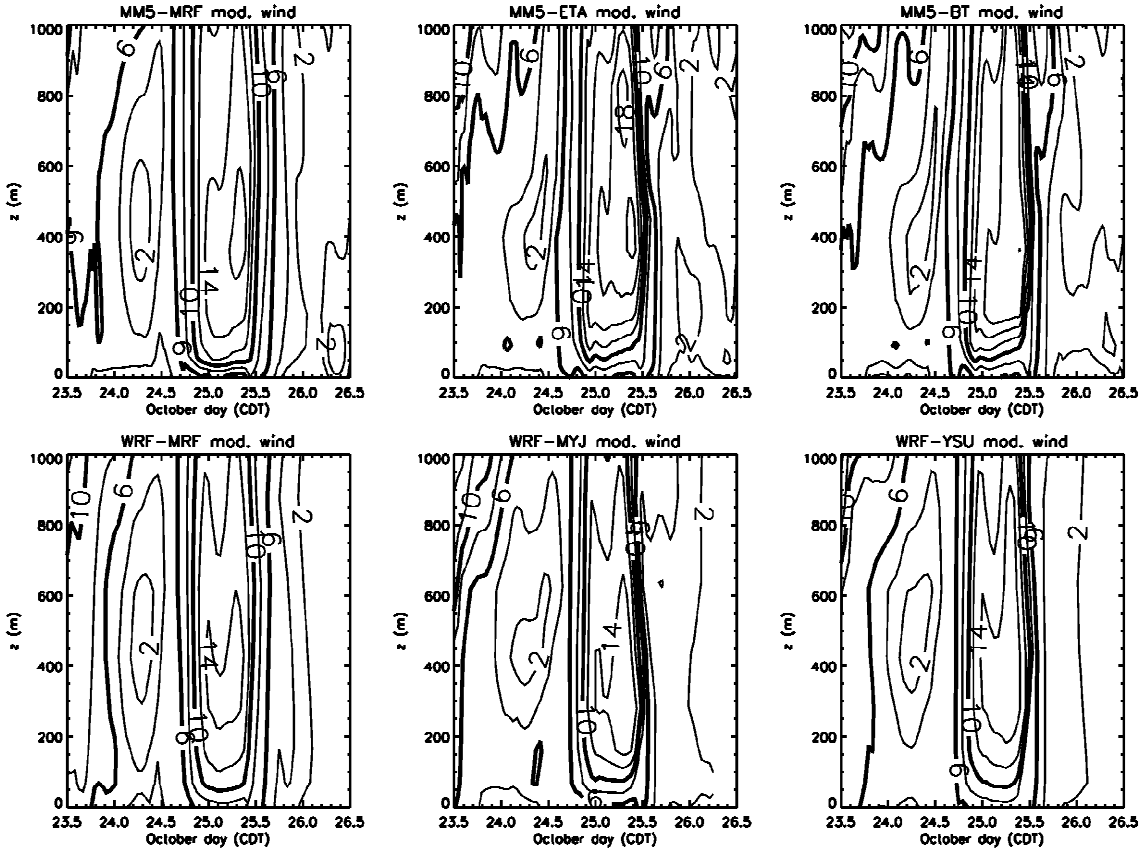

Fig. 5b: Contour plots of wind speed for different schemes in WRF and MM5. For COAMPS and HIRLAM these plots can be found in Steeneveld et al. (2008).

PART 2: Sensitivity study PBL schemes for stable conditions

Introduction

In this part of the study, we examine the sensitivity of the forecast of near surface variables for the formulation of the PBL parameterization in stable conditions. This is useful since the forecasting of stable conditions, especially under calm conditions (i.e. for wind speed less than 3 ms^{-1}) is problematic for NWP (see part I). Therefore, several alternative parameterizations for stable conditions have been implemented in the YSU scheme, since this scheme is the most complete and best performing scheme for daytime conditions. The sensitivity study was performed for the same case study in PART 1.
The investigated options are:

a) Default

The default version of WRF-YSU uses a prescribed eddy diffusivity (K) profile approach:

$$K = \frac{ku_* z}{\varphi_m}\left(1-\frac{z}{h}\right)^2 \qquad (2.1)$$

In which k is the Von Karman constant, z height, h PBL height, u_* the friction velocity and fm the stability function at the top of the surface layer. Amongst others, Steeneveld et al. (2008) showed that this

scheme overestimates the PBL mixing for calm and nighttime conditions, and therefore the following alternatives have been implemented and tested.

b) Local Monin-Obukhov theory (LMO):

$$K = (kz)^2 \left|\frac{\partial U}{\partial z}\right| (1 - 5Ri)^2 \qquad (2.2)$$

Herein Ri is the local Richardson number. This scheme is consistent with field observations of turbulence (e.g. Businger et al. 1971; De Roode and Duynkerke, 2000; Steeneveld 2007). In correspondence with these field observations, for Ri >0.2 the turbulence is set to 0, while the common approach in NWP is to allow for turbulent mixing for Ri > 0.2.

c) ECMWF-OLD:

$$K = (kz)^2 \left|\frac{\partial U}{\partial z}\right| f_{LTG}(Ri) \qquad (2.3)$$

This scheme has been in operation at the ECMWF since 1979 and is also used for the ERA40 project. The function f_{LTG}, that accounts for mixing efficiency reduction for large Ri, does allow, contrary to the LMO option, for mixing for Ri > 0.2. It even applies unrealistic large mixing for the PBL. A reduction of this reducing the mixing (as in Eq. (2.2)) degrades the ECMWF skill scores substantially.

d) ECMWF-NEW

$$K = \left(\left|\frac{\partial U}{\partial z}\right| + S(z)\right)\left(\frac{1}{kz\sqrt{f_{LMO}}} + \frac{1}{\lambda\sqrt{f_{LTG}}}\right)^{-2} \qquad (2.4)$$

As an attempt to reduce the mixing in the ECMWF-OLD scheme, recently this alternative has been implemented. The strategy behind this scheme is an interpolation between the ECMWF-OLD scheme and the LMO scheme. In addition a prescribed background shear function $S(z)$ was added to include effects of unresolved small scale baroclinicity.

Results

First we will focus on the impact of surface of the schemes on 10 m wind 2m temperature, friction velocity and PBL height. Fig 6 shows the difference between the new scheme and the original scheme for a representative situation. Panel a) shows that the introduction of YSU-LMO reduces the friction velocity with typically 0.1-0.2 ms^{-1}. This should be considered as an improvement, having in mind the overestimation of u_* in PART 1. PBL height are reduced in large parts of the model domain, although, probably due to interaction with the local orography, the PBL is modestly enlarged in a small part of the domain. Fig 6b shows a reduction of the 2m temperature in the whole domain, which is an improvement considering the overestimated surface temperatures in PART 1. Finally, 10 m wind speed is substantially reduced, which is a step forward in reducing the 10 wind speed high bias.

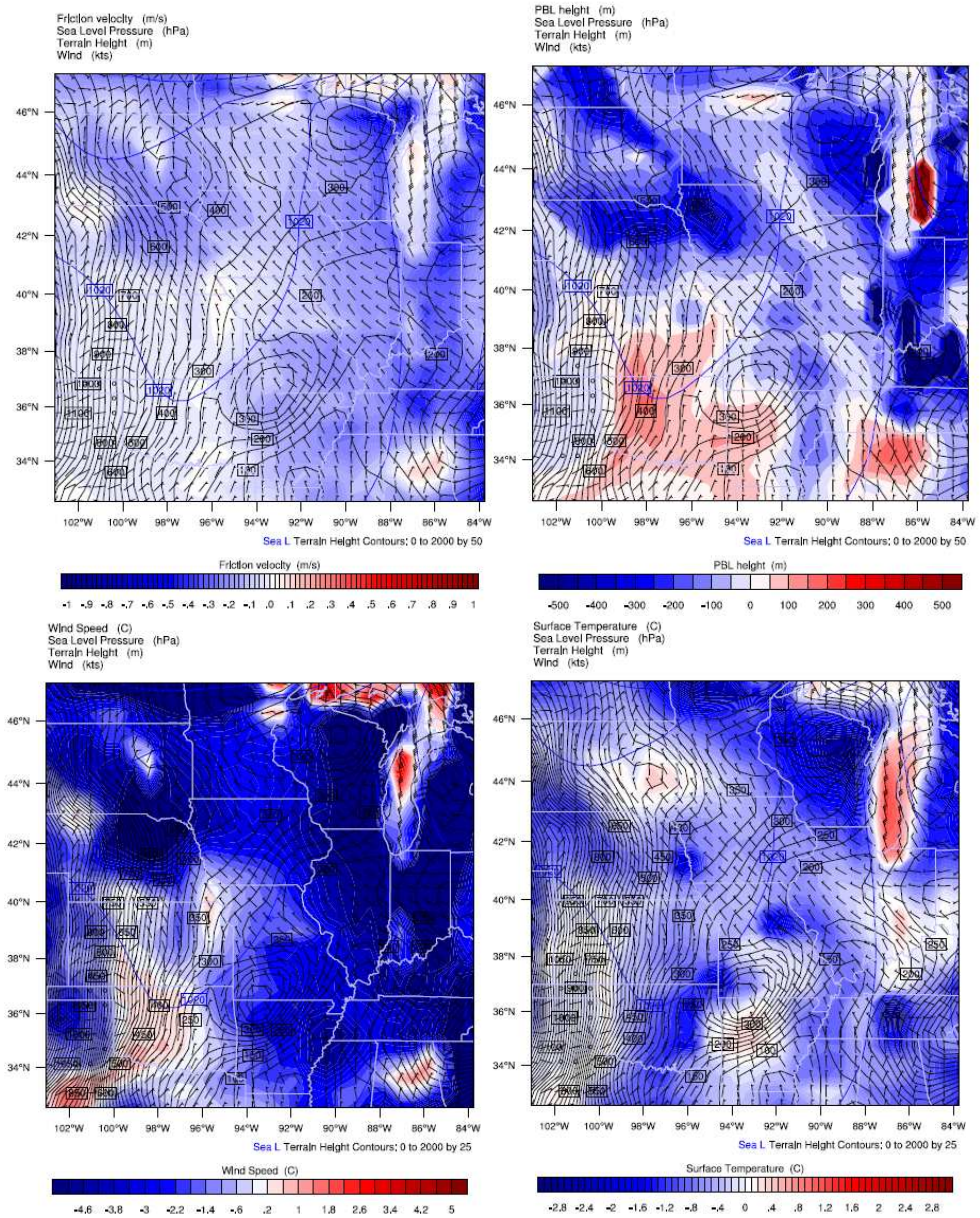

Fig. 6: difference plot for YSU-LMO – YSU-ORG for 23 Oct. 1999, 10.00 UTC for Great Plains region. a) Friction velocity, b) PBL height, c) 2m temperature, d) 10 m wind speed.

Fig. 7 shows the sensitivity of the new versus the old ECMWF stable PBL formulation. It is seen that for all near surface variables the differences are only minor, however in the direction of reduced bias. Keeping in mind the mentioned substantial biases with the old ECMWF scheme, such as overestimation of surface temperature, friction velocity, PBL depth and wind speed, one may not expect substantial improvement from the recent update at first glance. However, further testing on longer datasets and different atmospheric conditions is requested.

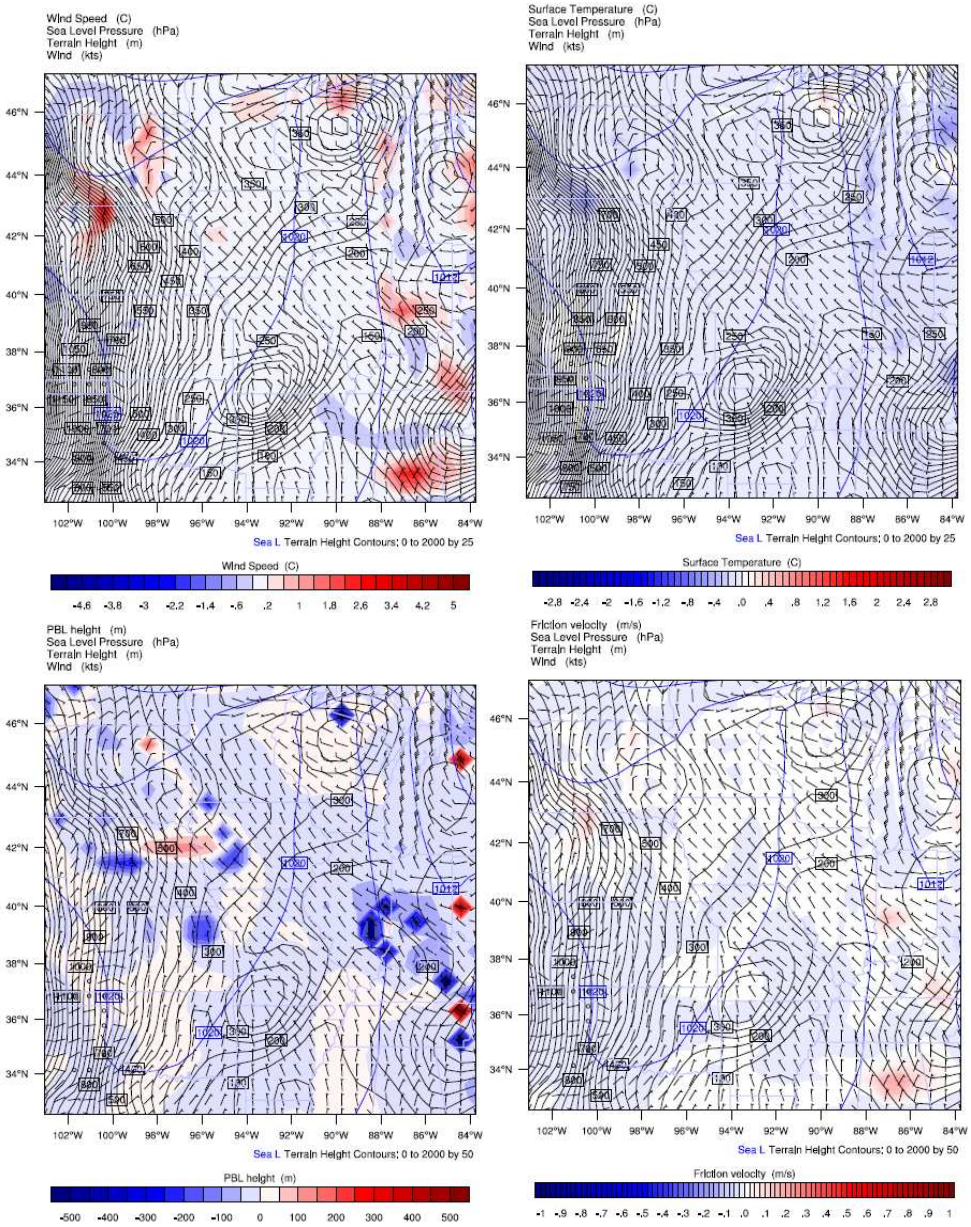

Fig. 7: difference plot for YSU-ECMWF-OLD – YSU-ECMWF-NEW for 23 Oct. 1999, 10.00 UTC for Great Plains region. a) Friction velocity, b) PBL height, c) 2m temperature, d) 10 m wind speed.

PART 3: Model validation against a network of scintillometers and ceilometers

Observations: BSIK network in the Netherlands.

The BSIK network (Fig. 8) in the Netherlands consists of detailed observations at the widely used 200 m tower in Cabauw (51.971ºN, 4.927ºE, -0.7 m ASL; Beljaars and Bosveld, 1997) for thermodynamic variables, turbulent and radiative surface fluxes, and turbulent fluxes (eddy covariance) at several levels in the 200 m tower. The site consists of a grass field in moist conditions (contrary to CASES-99). Besides the tower, new instruments providing much more detailed information are currently available. Those exist of surface sensible heat fluxes (H) on scales up to 10 kilometers that will be monitored using ***scintillometry*** (Hartogensis, 2006). This instrument measures turbulent surface fluxes along a path. This enables comparison with modeled grid cell averaged fluxes.

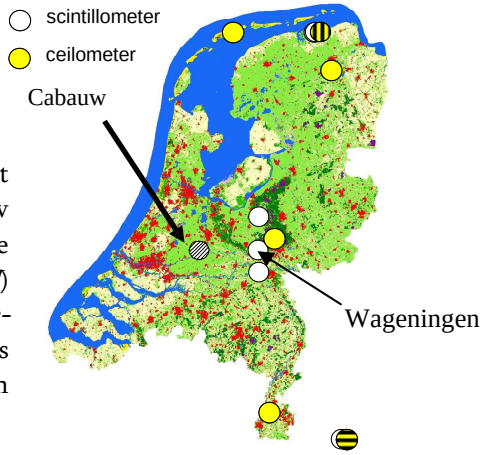

Fig 8: The Netherlands with spatial coverage of scintillometer and ceilometer network.

The research addresses the spatial variation of the ABL and its dynamics. The variation is monitored through a new operational network of optical scintillometers over different types of terrain (providing sensible heat fluxes), in combination with ceilometer data from a number of operational stations of KNMI (Royal Netherlands Meteorological Institute) (providing ABL height). This consortium of observations provides an innovative and unique opportunity for model evaluation. Thus, a virtually continuous record of ABL dynamics will be built against which we assess the performance of the boundary-layer schemes.

A scintillometer is an instrument that consists of a light transmitter and a receiver. The instrument records the integrated effect of the turbulent perturbations of the air's refractive index (n), and its structure parameters (C_n^2). Monin-Obukhov theory is used to convert C_n^2 to area-averaged surface fluxes of heat, using 10 m wind as input. We use 5 optical Large Aperture Scintillometers (LAS) which operate on a scale of ~500-5000m in regions of the Netherlands with different vegetation types (Fig. 8). See Meijninger et al. (2002) for more information on the LAS.

A ceilometer is an instrument that measures the ABL height (h) using laser or other light techniques. Fig. 8 also indicates 6 locations with operational ceilometers. In addition to this network of innovative instruments, we also evaluate the model against Cabauw tower observations (e.g. Beljaars and Bosveld, 1997), wind profiler, and routine micrometeorological observations.

MODEL SETUP & CASE DESCRIPTION

We have selected two cloud free contrasting days: 22 April 2007 (DOY 112) with weak winds (~1.5 ms^{-1} at 10m), and 2 May 2007 (DOY 122) with moderate winds (~4.5 ms^{-1} at 10m). During the first period, The Netherlands are located under a high with winds from the southeast. In the second period the wind is east-north-eastern. The area consists of mainly grassland and is flat and relatively homogeneous. Also, the area has a large water supply and thus a high soil moisture availability. For these simulations, the initial and boundary conditions (every 6 h) were provided by NCAR-FNL. WRF2.2 was run in an area of 1600 x 1600 km with a grid size of 54 km. In this domain, we nested 3 domains with a grid spacing of 18, 9 and 2 km respectively to minimize model errors due to lack of horizontal resolution (Fig. 9). Moreover, the U.S. Geological Survey provided the land surface properties for WRF such as soil moisture availability, surface roughness, and land use.WRF2.2 was run with 3 different ABL schemes. First, we use the so-called MRF scheme (Troen and Mahrt, 1986; Hong and Pan, 1996) which utilizes a prescribed cubic eddy diffusivity profile with height, with the magnitude depending on the characteristic velocity scale at the surface layer. This scheme allows for non-local heat transport during the day. This extension is needed to represent transport by large eddies on the scale of the ABL itself, instead of local transport. A well-known drawback of this widely used scheme is excessive daytime ABL top entrainment, and overestimation of the turbulent transport at night (e.g. Vila et al., 2004; Steeneveld et al., 2008).

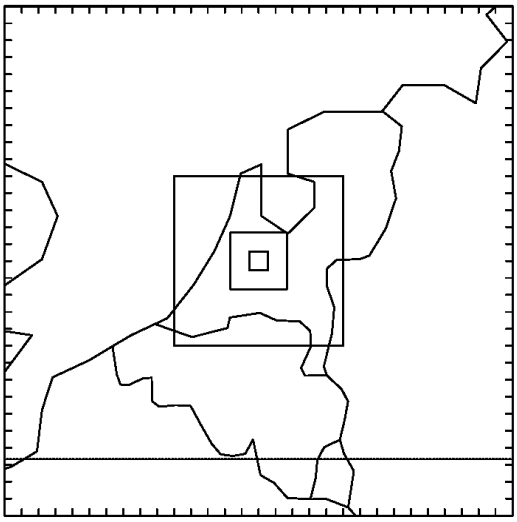

Fig 9: Model domain set-up. See text for further details

The 2nd scheme is an extension MRF, (so called YSU). The extensions consist of a) inclusion of prescribed entrainment rate at the ABL top, b) non-local transport of momentum, and c) Prandtl number (K_M/K_H) depending on height (see also Noh et al., 2003). As such, we will evaluate whether these modifications circumvent the deficiencies in the MRF scheme. Finally the 3rd scheme is a 1.5 order closure scheme (MYJ) and uses a prognostic equation for the turbulent kinetic energy (see Stull, 1988; Steeneveld et al., 2008). Then the eddy diffusivity is determined by multiplication of the turbulent kinetic energy and a length scale. The NOAH land surface scheme has been used (e.g. Ek et al., 2003). For completeness, we utilize the Kain-Fritsch cumulus convection scheme, the RRTM scheme for long wave radiation, the Dudhia scheme for shortwave radiation, and the WSM 3-class simple ice microphysics scheme. In the surface layer, we use Monin-Obukhov theory as in Janjic (1994).

a) Calm conditions: DOY 112

The modeled and observed H, latent heat flux (L_vE) and friction velocity (u_*) for Wageningen are shown in Fig. 10: all schemes overestimate daytime H by ~60 Wm^{-2}, while at night all schemes overestimate the magnitude of H. However, the scintillometer flux H_{sc} is larger compared to the eddy covariance (EC) flux H_{ec}, and closer to the model forecast. Note that H_{ec} for Cabauw is also shown for comparison. L_vE is forecasted correctly for the full diurnal cycle, and is also consistent with eddy covariance results. Unfortunately, all schemes predict a u_* factor 2 larger than observed during the day. At night u_* vanishes, while WRF keeps u_* at least 0.14 ms^{-1}. This might occur due to the model's relatively large roughness length (0.15 m), as advised for Cabauw (Beljaars and Holtslag, 1991). The surface skin temperature (T_s) is correctly forecasted during the day, but overestimated at night. This is due to the fact that incoming longwave radiation in MRF and YSU is overestimated by 5-10 Wm^{-2}. Finally, h is well represented by the ceilometer (at least for one algorithm). The ceilometer only records the nocturnal boundary layer during the second part of the night, but the daytime mixed layer and residual layer are well observed. Note that the modeled h was calculated from the modeled wind and temperature profile, using Troen and Mahrt (1986).

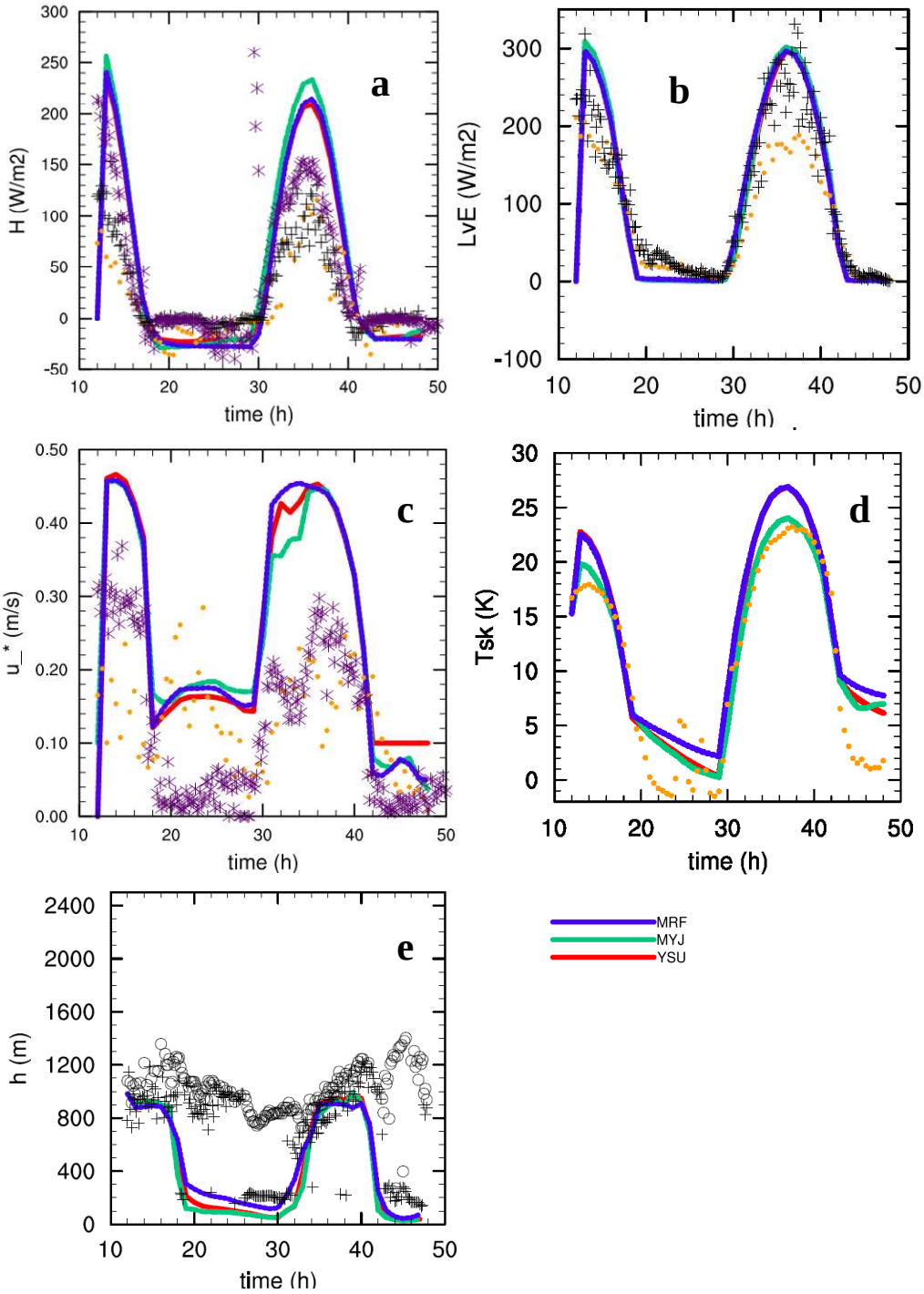

Fig.10: Modeled and observed time series of sensible (a), latent heat flux (b), friction velocity (c), surface skin temperature (d), and ABL height (e).+ Cabauw EC flux, ● = Wageningen EC flux, × Wageningen scintillometer flux. In panel e + and o refers to the first and second ABL structure change as seen by the ceilometer.

Fig. 11 shows the modeled profiles of θ, *q*, and *U*. For the daytime all ABL schemes overestimate the ABL temperature, although the near surface temperature agrees with the observations. Specific humidity is overestimated compared to the radio sounding, especially for MYJ.

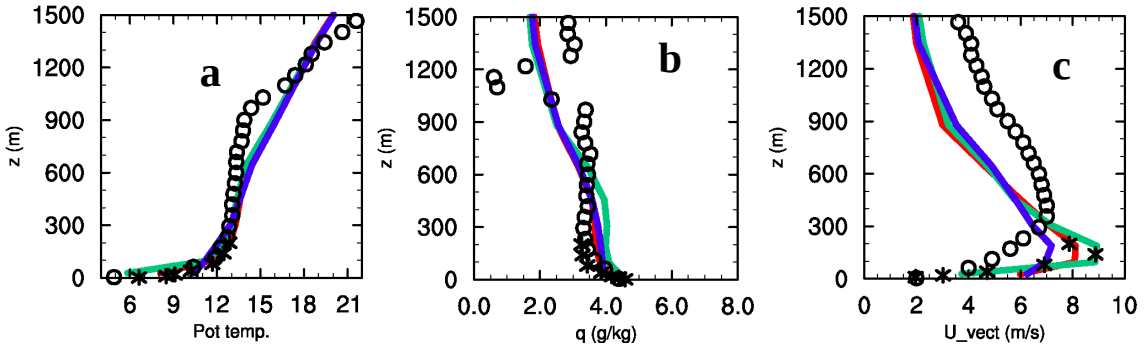

Fig.11: Modeled profiles of potential temperature, humidity, wind speed for DOY 112 2007,00 UTC. O = De Bilt sounding, X= Cabauw tower.

YSU seems to detrain more moisture compared to MRF. YSU seems to produce a much more well mixed U profile compared to MRF, which results in about 0.5 ms^{-1} wind speed difference. However, *U* is 1 ms^{-1} too high compared with tower observations and more compared to the sounding which we may consider suspicious close to the surface.

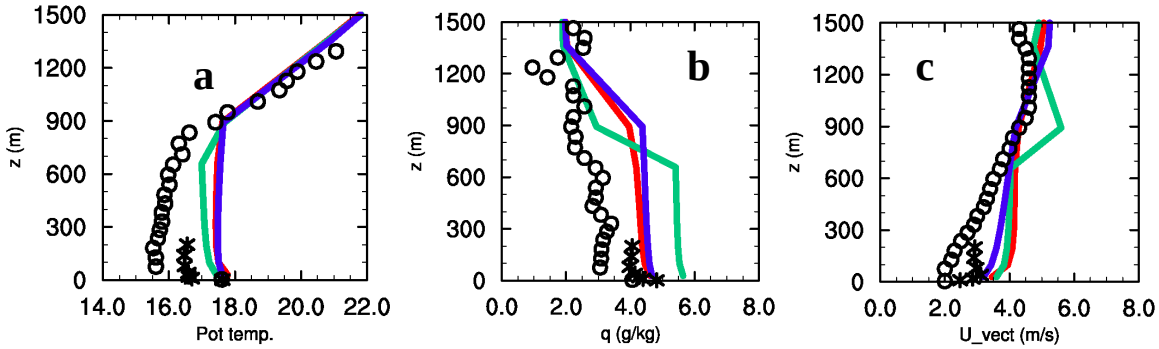

Fig. 12: Modeled potential temperature a), humidity (b), wind speed (c) for DOY 112 2007, 12UTC. O = radio sounding, asterisk is Cabauw tower.

At night (DOY 112, 00 UTC) the MYJ scheme reproduces the surface inversion correctly, while MRF and YSU underestimate the surface inversion strength, while also the free atmospheric stratification is underestimated. All schemes simulate *q* quite well close to the surface. For wind speed considerable differences are seen. MYJ represent the low level jet in very close agreement with tower observations. YSU forecasts the LLJ much better than MRF. This is due to YSU's larger near surface wind speed at daytime, which results in a larger amplitude of the inertial oscillation at night.

b) Windy conditions: DOY 122

Next we evaluate the model performance for DOY 122. The forecasted sensible heat flux is approximately similar for all schemes, and agrees well with H_{sc}. However, the daytime H_{sc} is much larger than H_{ec} in this case. It is also worth noting the clear peak of modeled and simulated *H* after the transition (Fig. 13).

The simulated L_vE is overestimated, although it compares well with the measured flux at Cabauw. WRF strongly overestimates u_*, especially for the day. Also note that u_* from the scintillometer iteration is substantially lower than from eddy covariance. Predicted T_s shows a cool bias at night, but is correct during the day. The daytime *h* is overestimated compared with the ceilometer observations. MRF overestimates *h* at night, compared to YSU and MYJ.

The simulated θ is underestimated, especially by MYJ (Fig. 14). This is inconsistent with the large surface *H*. Therefore, the modeled heat advection or entrainment is misrepresented. At the same time *q* is underestimated near the surface, and the wind speed profile is correctly modeled.

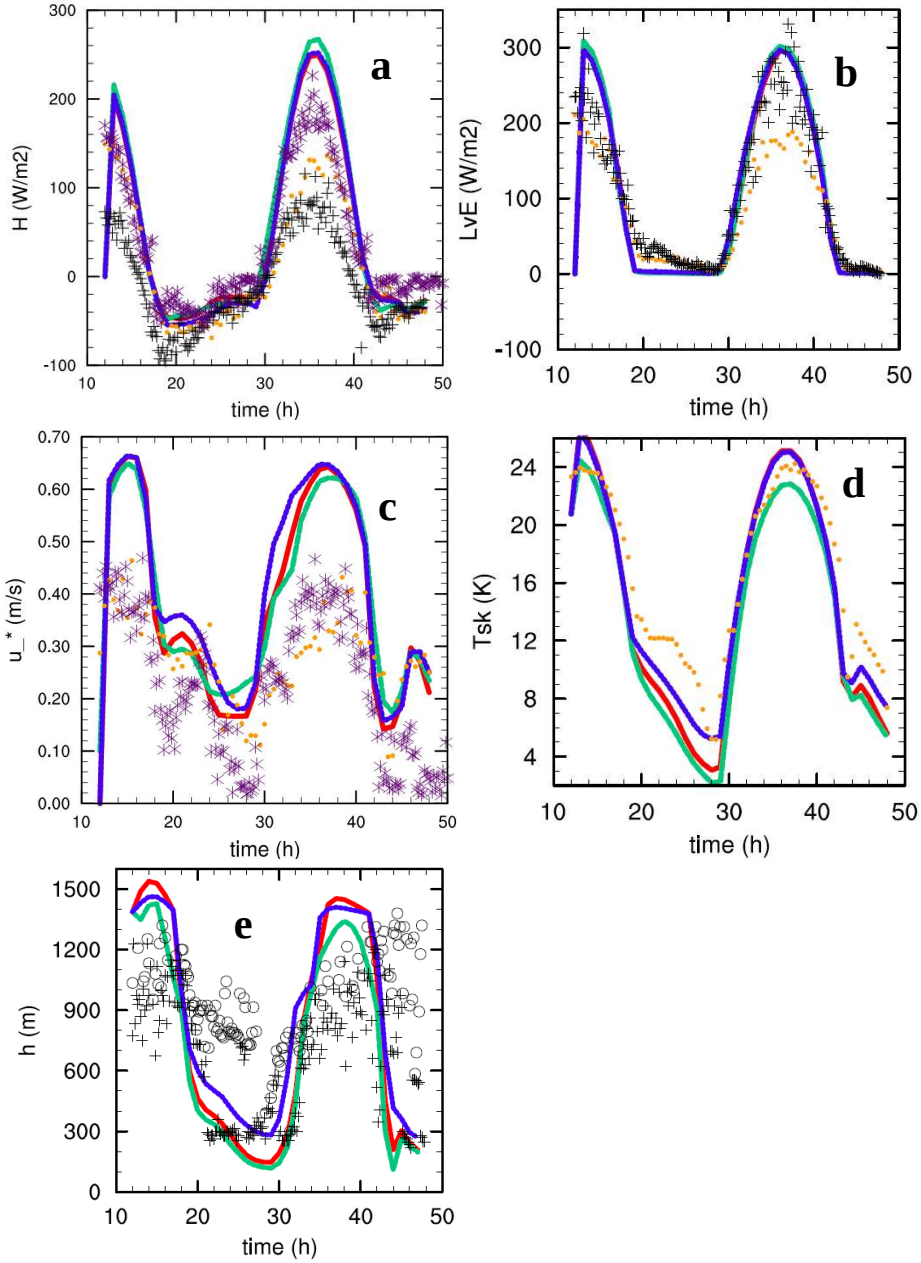

Fig.13: Modeled and observed time series of sensible (a), latent heat flux (b), friction velocity (c), surface skin temperature (d), and ABL height (e).+ Cabauw EC flux, ● = Wageningen EC flux, × Wageningen scintillometer flux. In panel e + and o refers to the first and second ABL structure change as seen by the ceilometer.

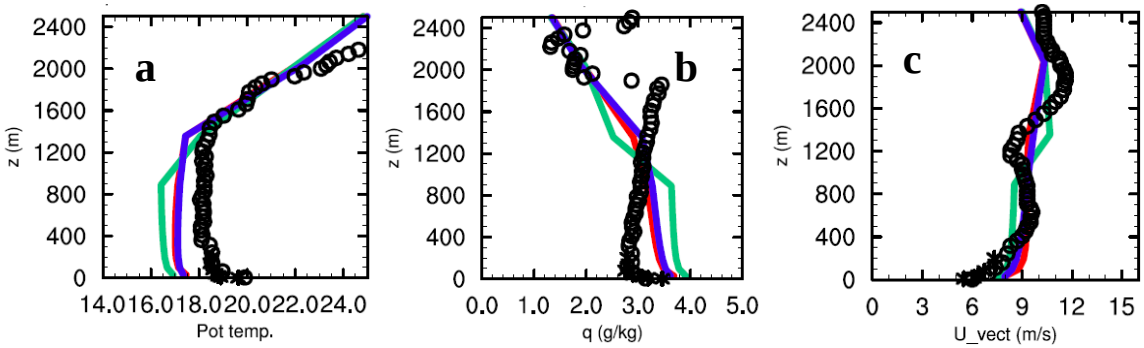

Fig.14: Modeled and observed potential temperature a), humidity (b), wind speed (c) for DOY 122 2007, 12UTC. o = radio sounding, asterisk is Cabauw tower.

4. CONCLUSIONS

We have added WRF model results in a model intercomparison study for the GEWEX Atmospheric Boundary Layer Study (GABLS). We found that WRF performs well against observations, but shows similar deficiencies as MM5, HIRLAM and COAMPS. As such further research on boundary layer parameterizations is required. As an alternative, we examined the sensitivity for WRF model results to the stable boundary layer parameterization. It was found that reducing the turbulent mixing in the stable boundary layer is beneficial for forecasts of near surface temperature, wind speed, friction velocity and boundary layer depth.

In addition, we have evaluated the model performance of WRF in the boundary layer against a network of ceilometers and scintillometers in the Netherlands. As such, this is the first evaluation in which grid scale model fluxes are compared with area averaged surface flux observations. The MRF, YSU and MYJ schemes are used. We find that the WRF-YSU scheme shows improved skill for the daytime wind profiles, and nighttime low-level jet compared to MRF. A common deficiency of the schemes is an overestimation of daytime sensible heat flux, and an overestimation of surface temperature at night for calm conditions.

Acknowledgements

The authors thank the BSIK-ME2 project (Climate changes spatial planning).

REFERENCES

Beare, R., M. MacVean, A. Holtslag, J. Cuxart, I. Esau, J-C. Golaz, M. Jimenez, M. Khairoutdinov, B. Kosovic, D. Lewellen, T. Lund, J. Lundquist, A. McCabe, A. Moene, Y. Noh, S. Raasch, and P. Sullivan, 2006: An intercomparison of Large-Eddy Simulations of the stable boundary layer, *Bound.-Layer Meteor.*, **118**, 247-272.

Beljaars A.C.M., F.C. Bosveld, 1997: Cabauw data for validation of land surface parametrization schemes. *J. Climate*, **10**, 1172-1193.

Beljaars, A., and P. Viterbo, 1998: Role of the boundary layer in a numerical weather prediction model, in *Clear and Cloudy boundary layers*, A.A.M. Holtslag,, P.G. Duynkerke Eds, Royal Netherlands Academy of Arts and Sciences, Amsterdam, 372p.

Businger, J.A., J.C. Wyngaard, Y. Izumi and E.F. Bradley, 1971: Flux profile Relationships in the Atmospheric Surface Layer*, J. Atmos. Sci*, **28**, 181-189.

Cheng, W.Y.Y., W.J. Steenburgh, 2005: Evaluation of surface sensible weather forecasts by the WRF and Eta models over the western United States. *Wea. For.*, **20**, 812-821.

Denning, S.A., N. Zhang, C. Yi, M. Branson, K. Davis, J. Kleist, P. Bakwin, 2008: Evaluation of modeled atmospheric boundary layer depth at the WLEF tower. *Agric. For. Meteor.*, **148**, 206-215.

Duynkerke, P.G. and S. de Roode, 2001: Surface energy balance and turbulence characteristics observed at the SHEBA Ice Camp during FIRE III, *J. Geo. Res.*, **106**, D4, 15313-15322.

Ek, M.B., K.E. Mitchell, Y. Lin, E. Rogers, P. Grunmann, V. Koren, G. Gayno, J.D. Tarpley, 2003, Implementation of the Noah land surface model advances in the National Centers for Environmental Prediction operational mesoscale Eta model. *J. Geophys. Res.*, **108** (D22), 8851, doi:10.1029/2002JD003296.

Gerbig, C., S. Körner, J.C. Lin, 2008: Vertical mixing in atmospheric tracer transport models: error characterization and propagation. *Atmos. Chem. Phys.*, **8**, 591-602.

Ha, K.J. and L. Mahrt, 2003: Radiative and turbulent fluxes in the nocturnal boundary layer, *Tellus,* **55A**, 317-327.

Hanna, S.R. and R. Yang, 2001: Evaluation of meso scale models' simulations of near-surface winds, temperature gradients, and mixing depths, *J. Appl. Meteor.*, **40**, 1095-1104.

Hartogensis, O.K., 2006: *Exploring Scintillometry in the Stable Atmospheric Surface Layer*, Wageningen Univ., PhD Thesis, 228p.

Holtslag, A.A.M., 2006: Special issue for boundary-layer meteorology: GEWEX Atmospheric Boundary-Layer Study (GABLS) on stable boundary layers, *Bound.-Layer Meteor.*, **118**, 243-246.

Holtslag, A.A.M. and H.A.R. de Bruin, 1988: Applied modelling of the nighttime surface energy balance over land, *J. Appl. Meteor.*, **27**, 689-704.

Holtslag, A.A.M., E. van Meijgaard, and W.C. de Rooy, 1995: A comparison of boundary layer diffusion schemes in unstable conditions over land, *Bound.-Layer Meteor.*, **76**, 69-95.

Hong, S.Y. and H.L. Pan, 1996: Nonlocal boundary layer vertical diffusion in a Medium-Range Forecast model. *Mon. Wea. Rev.*, **124**, 2322-2339.

Janjić, Z.I., 1994: The step-mountain coordinate model: Further developments of the convection, viscous sublayer, and turbulence closure schemes. *Mon. Wea. Rev.*, **122**, 927-945.

King, J.C., W.M. Connolley and S.H. Derbyshire, 2001: Sensitivity of modelled Antarctic climate to surface flux and boundary-layer flux parameterizations, *Quart. J. Roy. Meteor. Soc.,* **127**, 779-794.

Mahrt, L., 1999: Stratified atmospheric boundary layers, *Bound.- Layer Meteor.*, **90**, 375-396.

Meijninger, W.M.L., O.K. Hartogensis, W. Kohsiek, J.C.B. Hoedjes, R.M. Zuurbier, H.A.R. DeBruin, 2002: Determination of area-averaged sensible heat fluxes with a large aperture scintillometer over a heterogeneous surface-Flevoland field experiment. *Bound.-Layer Meteor.*, **105**, 37-62.

Miao, J.-F., D. Chen, K. Borne, 2007: Evaluation and comparison of Noah and Pleim-Xiu Land Surface Models in MM5 using GÖTE2001 data: spatial and temporal variations in near surface air temperature. *J. Appl. Meteor. Clim.*, **46**, 1587-1605.

Noh, Y., W.G. Cheon, S.Y. Hong, S. Raasch, 2003: Improvement of the K-profile model for the planetary boundary layer based on large eddy simulation data. *Bound.-Layer Meteor.*, **107**, 401-427.

Olivié, D.J.L., P.F.J. van Velthoven, A.C.M. Beljaars, 2004: Evaluation of archived and off-line diagnosed vertical diffusion coefficients from ERA-40 with ^{222}Rn simulations. *Atmos. Chem. Phys.*, **4**, 2313-2336.

Poulos, G.S., and co-authors, 2002: CASES-99: A comprehensive Investigation of the stable nocturnal boundary layer, *Bull. Amer. Meteor. Soc.*, **83**, 555-581.

Räisänen, P., 1996: The effect of vertical resolution on clear-sky radiation calculations: test with two schemes, *Tellus*, **48A**, 403-423.

Song, J., K. Liao, R.L. Coulter and B. M. Lesht, 2005: Climatology of the Low-Level Jet at the Southern Great Plains Atmospheric Boundary Layer Experiments Site, *J. Appl. Meteor.*, **44**,1593-1606.

Steeneveld, G.J., 2007: Understanding and Prediction of Stable Atmospheric Boundary Layers over Land. PhD Thesis, Wageningen Univ. Wageningen, Netherlands, 199p.

Steeneveld, G.J., B.J.H. van de Wiel, and A.A.M. Holtslag, 2006: Modeling the Evolution of the Atmospheric Boundary Layer Coupled to the Land Surface for Three Contrasting Nights in CASES-99, *J. Atmos. Sci.*, **63**, 920-935.

Steeneveld, G.J., T. Mauritsen, E.I.F. de Bruijn, J. Vilà-Guerau de Arellano, G. Svensson, A.A.M. Holtslag, 2008: Evaluation of limited area models for the representation of the diurnal cycle and contrasting nights in CASES99. *J. Appl. Meteor. Clim.* **47**, 869-877.

Stull, R.B, 1988: *An Introduction to Boundary-layer Meteorology*, Kluwer Academic Publishers, Dordrecht, 666 pp.

Svensson, G., and A.A.M. Holtslag, 2007: The diurnal cycle-GABLS second intercomparison project. *GEWEX news*, February.

Svensson, G., and A.A.M. Holtslag, 2006: Single column modeling of the diurnal cycle based on CASES99 data – GABLS second intercomparison project, *17th Symposium of Boundary Layers and Turbulence*, 22-25 May 2006, San Diego, U.S.A. American Meteor. Soc. Boston, P8.1.

Teixeira, J., B. Stevens, C.S. Bretherton, R. Cederwall, J.D. Doyle, J.C. Golaz, A.A.M. Holtslag, S.A. Klein, J.K. Lundquist, D.A. Randall, A.P. Siebesma, and P.M.M. Soares, 2008 : Parameterization of the Atmospheric Boundary Layer-A View from Just Above the Inversion. *Bull. Amer. Meteor. Soc.*, **89**, 453-458.

Tie, X., S, Madronich, G. Li, Z. Ying, R. Zhang, A.R. Garcia, J. Lee-Taylor, and Y. Liu, 2007: Characterizations of chemical oxidants in Mexico City: A regional chemical dynamical model (WRF-Chem) study. *Atmos. Environ*, **41**, 1989-2008.

Troen, I.B. and L. Mahrt, 1986: A simple model of the atmospheric boundary layer; sensitivity to surface evaporation, *Boundary-Layer Meteor.*, **37**, 129-148.

Vila, J., P. Casso-Torralba, 2007: The radiation and energy budget in mesoscale models: an observational study case. *Física de la Tierra*, **19**, 117-132.

Vilà-Guerau de Arellano, J. B. Gioli, F. Miglietta, H. J. J. Jonker, H. K. Baltink, R. W. A. Hutjes, and A. A. M. Holtslag, 2004: Entrainment process of carbon dioxide in the atmospheric boundary layer, *J. Geophys. Res.*, **109**, D18110, doi:10.1029/2004JD004725

Wiel, B.J.H. van de, R.J. Ronda, A.F. Moene, H.A.R. de Bruin and A.A.M. Holtslag, 2002: Intermittent turbulence and oscillations in the stable boundary layer over land. Part I: A bulk model, *J. Atmos. Sci.*, **59**, 942-958.

Zehnder, J.A., 2002: Simple modifications to improve Fifth-Generation Pennsylvania State University-National Center for Atmospheric Research Mesoscale Model performance for the Phoenix, Arizona, Metropolitan Area, *J. Appl. Meteor.*, **41**, 971-979.

Zhong, S., H. In, C. Clements, 2007: Impact of turbulence, land surface, and radiation parameterizations on simulated boundary layer properties in a coastal environment. *J. Geophys. Res.*, **112**, doi:10.1029/2006JD008274.